Gel Permeation Chromatography Calibration Based on Fractal Geometry

A. G. Boborodea,[1] M. Clemens,[2] D. Daoust,[1] C. Bailly[1]

[1]*Unité de Physique et de Chimie des Hauts Polymères, Université catholique de Louvain, Bâtiment Boltzmann, Place Croix du Sud, 1 B-1348 Louvain-la-Neuve, Belgium*
[2]*Department of Chemistry and Materials, Manchester Metropolitan University, John Dalton Building, Chester Street, Manchester, M1 5GD, UK*

Received 22 August 2003; accepted 28 January 2004
DOI 10.1002/app.20550
Published online in Wiley InterScience (www.interscience.wiley.com).

ABSTRACT: The previously developed model [Polym Bull 2000, 44, 525] used to characterize the porous gel inside a gel permeation chromatography (GPC) column, has been extended to also include the interstitial space between the macroscopic gel particles. The hydrodynamic dimensions for 12 polystyrene (PS) standards, measured by GPC with differential refractive index (DRI), differential viscometry (VISCO), and multiangle laser light scattering (MALLS) detectors, have been used to determine the fractal parameters of the polystyrene–divinylbenzene gel corresponding to four commercial columns. The new developed model enables to predict the calibration curve for the sets of coupled columns based on the parameters of each column. © 2004 Wiley Periodicals, Inc. J Appl Polym Sci 93: 771–777, 2004

Key words: gel permeation chromatography (GPC); light scattering; modeling

INTRODUCTION

After the publication of the book by Mandelbrot,[1] fractals have found many theoretical and practical applications in different domains of science and technology. A specific interest was developed for the characterization of porous media,[2–4] which frequently exhibit self-similar properties at different scales of length.[5,6] In the case of controlled-porosity polymer absorbents, the applications in separation processes[7,8] determined the development of methods to measure the fractal parameters by sorption of water vapor,[9] transmission electron microscopy,[10] or small-angle neutron scattering.[10,11] For crosslinked styrene–divinylbenzene gel particles, the pore structure was found to be associated with voids and crevices located between the microgel particles.[11]

For gel permeation chromatography (GPC), a technique used for the separation of macromolecules by size, usually small (5–10 μm) spherical particles with narrow size distribution of pores are desirable.[12] In the classical theory of GPC,[13–15] the separation mechanism is governed primarily by the equilibrium distribution of solute species between the mobile solution phase and the solution within pores of macromolecular size. For flexible chain polymers, the distribution (or partition) coefficients, K_d, are calculated for random flight chains in cavities of simple geometrical forms (sphere, cylinder, or slab) with rigid impermeable and noninteractive walls. The K_d value is identified with the effective fraction of pore volume available to the solute in a chromatographic column to compare the theoretical calculations with the experimentally determined elution volumes.[16] Therefore, each fraction of the injected polymer sample, corresponding to macromolecules with gyration radius R_g, is separated at a retention or elution volume V_r, equal with the volume available for that fraction in the chromatographic column:

$$V_r = V_0 + K_d V_P \qquad (0 \le K_d \le 1), \tag{1}$$

where V_0 is the interstitial volume and V_P is the internal volume of pores inside of the column. For a certain polymer fraction characterized by R_g, the value of (K_d V_P) is the cumulative volume determined by the pores of the gel with an accessible diameter larger or equal to R_g.

There are two limiting cases to be considered.

The first limiting case, where $K_d = 0$, the molecules are totally excluded from the pores (their hydrodynamic dimensions are superior to the pores diameter) and:

$$V_r = V_0. \tag{2}$$

For this reason, V_0 is called total exclusion volume. All the molecules totally excluded emerge at the same

Correspondence to: A.G. Boborodea (boborodea@poly.ucl.ac.be).

moment from the column, after the flowing of a liquid volume equal to the interstitial volume.

The second limiting case, where $K_d = 1$, all the pores of the stationary phase allow access for the sample molecules and:

$$V_r = V_0 + V_P = V_T, \tag{3}$$

where V_T is called total permeation volume.

Experimentally, V_0 and V_T are considered as the lower and upper limits of the linear relationship between the molecular mass logarithm and the retention volume, and can be measured by injecting a series of polymer standards. This linear region corresponds to the selective permeation of the macromolecules having dimensions comparable with the pore diameter.

However, experimentally it was observed that some separation still exists for macromolecular masses outside the domain of the selective permeation. To explain this separation for the permeating particles smaller than the pore dimension, the theory was extended by considering that the effectively accessible volume fraction of the cavity is determined by two factors: its surface per unit volume and a characteristic length of the permeating species.[16] Together, these values give the volume of a layer adjacent to the cavity walls that must be subtracted from the actual volume.

Starting from this idea and using the theory of Brochard-Wyart,[17] we have previously obtained the following relationship for K_d to characterize the tri-dimensional gel inside the chromatographic column:[18]

$$K_d = 1 - \left(\frac{R_g}{L}\right)^{3-d_f}, \tag{4}$$

where L is the linear size and d_f is the fractal dimension of the pores. In the fractal theory, the separation is governed by the same mechanism for both small chains and macromolecules having R_g comparable with the pore dimension. Because of the scale independence of the fractal dimension, d_f is used to calculate the surface per unit volume corresponding to all polymer species. Also, R_g is used as the characteristic length to calculate the volume of the layer adjacent to the pore cavities, which have a volume equal to L^3.

The obtained equation for K_d explains the decreasing power of separation for low molecular masses. In other words, a linear relationship is obtained for $\ln(1 - K_d)$ vs $\ln(R_g)$ for molecular masses smaller than a certain value. This limiting value corresponds to a macromolecular chain having a radius of gyration equal to the upper cutoff characteristic length of the porous gel:

$$R_{g,\max} = L. \tag{5}$$

For practical reasons, the definition of V_T must be extended to contain all low molecular mass fractions. Therefore, V_T value is considered as the elution volume corresponding to the solvent peak.

The difference between the classical theory and the fractal theory consists in the way the porous gel is described. In the classical theory, the size and the shape of the pore are defined by two geometrical parameters in function of the considered pore model. These two parameters define the selective permeation domain, and therefore give the linear relationship between K_d and the logarithm of the molecular mass or radius of gyration. In the fractal theory the pore shape is described by a fractal dimension. The separation is governed by the available pore surface for a certain macromolecular chain. The scale invariance of fractal objects also gives the possibility to take into account the separation of small molecules, which are considered by the classical theory as totally permeable into the pores.

The great disadvantage of the developed fractal theory is that the molecular mass corresponding to the limiting value determined by eq. (5) is usually lower than the upper limit where the separation is actually recorded. This additional unexplained separation is the main limitation to the use of the theory for the prediction of the calibration for sets of coupled columns.

In this article, to remove the limitation, we extend the fractal theory to include the interstitial space between the gel particles inside the column. Based on new derived equations we calculate the fractal parameters for four commercial columns using the gyration radius values measured for 12 polystyrene (PS) standards by GPC with multiangle laser light scattering (MALLS), differential refractive index (DRI), and viscometric (VISCO) detectors. This allows us to find relationships to construct the universal calibration for the set of the coupled columns based on parameters determined for each column.

THEORY

To account for the experimental fact that chains having a gyration radius much greater than the linear pore dimension are still separated by the GPC column, we include in the definition of V_P the volume corresponding to the macroscopic interparticle porosity. Experimentally, this is reflected in the V_0 value, which is now smaller than the previous value, and corresponds to the peak onset of a very high molecular mass sample.

Using the same definition for K_d given by relationship (4), we now introduce two scales for the porous gel inside the column.

A first scale, for low molecular masses, corresponds to the pores, and is determined as in original fractal theory by the following equation:

$$K_d = K_{d,P} = 1 - \left(\frac{R_g}{L_P}\right)^{3-d_P}, \quad (6)$$

where d_P and L_P represent the fractal and the linear dimensions of the pores.

For polymers having high molecular masses, the separation is determined by the interparticle space and the scale is modified. The partition coefficient is given by:

$$K_d = K_{d,G} = 1 - \left(\frac{R_g}{L_G}\right)^{3-d_G}, \quad (7)$$

where d_G and L_G represent the fractal and the linear dimension of interparticle space of the macroscopic gel. Characterizing the distance between gel particles, L_G also gives the highest value of the radius of gyration, which can be analyzed without blocking the column.

Experimentally, K_d is a continuous function of R_g. Imposing the condition that $K_{d,P} = K_{d,G}$, from eqs. (6) and (7) we can find the molecular size R_S corresponding to the switch between pore and interparticle separation regimes:

$$R_S = \left(\frac{L_P^{3-d_P}}{L_G^{3-d_G}}\right)^{1/(d_G-d_P)} \quad (8)$$

We can assume that columns having particles with the same diameter must have identical d_G and L_G values. In other words, a single linear relationship must be obtained by representing $\ln(1-K_d)$ vs $\ln(R_g)$ for polymers with $R_g > R_S$ corresponding to different columns with the same particle diameter.

Once K_d is defined for one column for all domains of elution volumes, we can derive the relationship for a set of n columns.

For the column set, the partition coefficient is defined by the following relationship:

$$K_d = \frac{V_r - V_0}{V_T - V_0}, \quad (9)$$

where V_r, V_T, and V_0 are calculated now for the total set of columns. We assume that:

$$V_r - V_0 = \sum_{i=1}^{n}(V_{r,i} - V_{0,i}), \quad (10)$$

and

$$V_T - V_0 = V_P = \sum_{i=1}^{n} V_{P,i}. \quad (11)$$

The relationships (10) and (11) are true only for chromatographic systems that have connection tubing between injector, columns, and detectors of negligible volumes.

Introducing the relationships (10) and (11) in eq (9) we obtain:

$$K_d = \frac{1}{\sum_{i=1}^{n} V_{P,i}} \sum_{i=1}^{n}(V_{P,i}K_{d,i}), \quad (12)$$

where for column i, the value for $K_{d,i}$ is given by the following equation:

$$K_{d,i} = \frac{V_{r,i} - V_{0,i}}{V_{P,i}} = \begin{cases} 1 - \left(\frac{R_g}{L_{P,i}}\right)^{3-d_{P,i}} & \text{for } R_g \le R_{S,i} \\ 1 - \left(\frac{R_g}{L_{G,i}}\right)^{3-d_{G,i}} & \text{for } R_g > R_{S,i} \end{cases}. \quad (13)$$

Equations (12) and (13) allow the construction of a GPC calibration for a column set based on parameters obtained separately for each column in the set.

If the columns are characterized by almost identical volumes, $V_{P,i}$, the relationship (12) could be simplified to:

$$K_d = \frac{1}{n}\sum_{i=1}^{n} K_{d,i}. \quad (14)$$

EXPERIMENTAL

The chromatograms for 12 narrow molecular mass distribution PS standards, listed in Table I, were recorded using an Alliance GPCV 2000 Waters chromatograph equipped with a differential refractive index detector (DRI) and a viscometer detector (VISCO). A Wyatt Dawn DSP 18-angle laser light-scattering detector (MALLS) was introduced between the column set and the DRI detector. The following operational conditions were adopted. The polymer solutions were prepared at room temperature in tetrahydrofuran (THF, HPLC quality, Fluka) at concentrations between 0.5 to 1.5 mg/mL. A volume of 215.5 μL was injected at room temperature, 25°C. The flow rate was fixed at 1.0 mL/min. The measured interdetector volumes were 0.183 mL between the MALLS and the DRI detectors and 0.041 mL between the DRI and the VISCO detectors. The VISCO detector was calibrated for the operating flow rate using the internal proce-

TABLE I
Polystyrene Standards

No.	PS standard	M_{peak} (g/mol)	M_w/M_n
1	PS 1660[a]	1660	1.06
2	PS 5000[a]	5000	1.03
3	PS 7000[a]	7000	1.04
4	PS 9860[a]	9860	1.02
5	PS 37900[b]	37,900	1.01
6	PS 76600[a]	76,600	1.03
7	PS 186000[a]	186,000	1.03
8	PS 426600[a]	426,600	1.03
9	PS 706000[b]	706,000	1.05
10	PS 1226000[a]	1,226,000	1.04
11	PS 3390000[a]	3,390,000	1.06
12	PS 5480000[b]	5,480,000	1.15

[a] Polymer Laboratories.
[b] Tosoh Corporation.

dure of the Alliance GPCV 2000. The Rayleigh constant for the MALLS was determined using toluene (HPLC quality, Lab Scan) and the internal procedure of the DAWN DSP detector. To eliminate any contamination, an in-line filtration using a sterile filter (Anatop 25, 0.02 μm, Whatman) was used to inject toluene into the DAWN cell. The Rayleigh constant for THF was automatically calculated by the Astra Version 4.7 software (Wyatt Technology), using the refractive index values for toluene (1.491) and THF (1.403). The normalization of the Dawn photometer detectors was performed with the PS 37900 standard, which did not show angular dependence on the light scattering signal.

The characterization of the polymer standards was performed using a set of four Waters Styragel columns (HR2, HR3, HR4, and HR5). The obtained hydrodynamic dimensions were used to characterize each column in the set. The experiments were performed for the single columns as well as for the coupled set of columns.

RESULTS AND DISCUSSION

Hydrodynamic dimensions of PS standards

The DRI-VISCO detector combination allows the determination of the intrinsic viscosity of each molecular mass increment in the distribution. For narrow distribution PS standards, the average intrinsic viscosity value $[\eta]$ has been automatically calculated by the Millennium software based on the peak areas recorded with both detectors. For the PS standards listed in Table I, the average hydrodynamic volumes, $V_h = [\eta]M_{peak}$, have been calculated using the molecular mass corresponding to the peak apex, M_{peak}.

Using the Zimm method and from the angular dependence of the intensity of the scattered light, it is possible to calculate the root mean square radii of gyration $\langle R_g^2 \rangle^{1/2}$ for each slice across the sample chromatographic peak. These values are further averaged to obtain the radius of gyration. The data manipulation has been carried out by the Astra software. Because the intensity of the scattered light is proportional to the molecular mass of the polymer, the sensitivity of the method decreases for lower molecular masses, high level of errors (more than 25%) being recorded for PS standards having $M_{peak} < 30$ kg/mol.

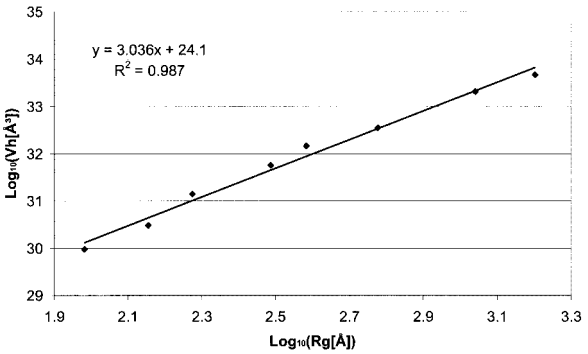

Figure 1 Log_{10}–Log_{10} plot of the hydrodynamic volume vs the radius of gyration, for PS standards having $M_{peak} > 30$ kg/mol.

The relationship between the average hydrodynamic volume determined by DRI-VISCO, and the average radius of gyration, measured by DRI-MALLS, is presented in Figure 1 for PS standards having $M_{peak} > 30$ kg/mol. The obtained slope is close to the theoretical value of 3.

Determination of the column parameters

For all columns and the column set, the V_T values were considered as the eluting volumes corresponding to the solvent peak and the V_0 values were considered as the volume corresponding to the onset of the PS 5480000 peak, given by the DRI detector. The results are presented in Table II. The fact that the internal volume for the column set is given by the sum of the internal volumes of each column in the set confirms that the connection tubing between the columns has a very small volume. The V_0 and V_T volumes obtained by summing the volumes correspond-

TABLE II
Column Volumes

Column	V_0 (mL)	V_T (ml)	V_P (mL)
HR2	4.7	12.6	7.9
HR3	4.4	12.5	8.1
HR4	4.3	12.5	8.2
HR5	5.6	13.4	7.8
Total	19.0	51.0	32.0
Column set	18.4	50.4	32.0

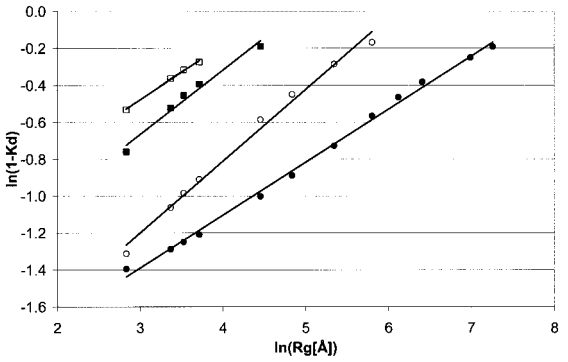

Figure 2 $\ln(1-K_d)$ vs $\ln(R_g$ [Å]) in THF at 25°C for PS standards selected in Table III for the following columns: HR2 (□), HR3 (■), HR4 (○), HR 5(●).

ing to each separate column are slightly higher than the volumes obtained for the column set. This is due to the fact that for each column as well as for the column set, the measured volume V_0 (or V_T) using DRI detector, contains both the actual volume and the interdetector volume between MALLS and DRI. Because the set contains four coupled columns, the V_0 (or V_T) obtained by summing the volumes corresponding to each separate column contains four times the interdetector volume. In the measured V_0 (or V_T) for the column set, the interdetector volume is counted only one time. The third part of the difference between V_0 (or V_T) obtained by summing the volume for each column and the corresponding value measured for column set is equal to 0.2 mL. This is close to the measured interdetector volume between the MALLS and the DRI detectors, 0.183 mL.

To calculate the fractal parameters d_P and L_P for each column, the relationship (6) may be rewritten as:

$$1 - K_d = \left(\frac{R_g}{L_P}\right)^{3-d_P}. \quad (15)$$

TABLE III
PS Standards Selected (X) to Calculate the Fractals Parameters Corresponding to the Pore Separation for Different Columns

PS standard	HR2	HR3	HR4	HR5
PS 1660	X	X	X	X
PS 5000	X	X	X	X
PS 7000	X	X	X	X
PS 9860	X	X	X	X
PS 37900	—	X	X	X
PS 76600	—	—	X	X
PS 186000	—	—	X	X
PS 426600	—	—	X	X
PS 706000	—	—	—	X
PS 1226000	—	—	—	X
PS 3390000	—	—	—	X
PS 5480000	—	—	—	X

TABLE IV
Fractal Parameters L_P and d_P for Each Column

Column	d_P	L_P (nm)
HR2	2.70	10.0
HR3	2.65	13.7
HR4	2.61	44.0
HR5	2.71	256

By taking logarithms, a linear relationship between the radius of gyration and $(1-K_d)$ results:

$$\ln(1 - K_d) = (3 - d_P)\ln(R_g) - (3 - d_P)\ln(L_P). \quad (16)$$

In Figure 2, we present the part corresponding to the pore separation of the calibration curves for the four GPC columns. The PS standards selected for this separation for each GPC column are given in Table III. This linear domain of the calibration curve was used to calculate the fractal parameters, L_P and d_P, for each column based on eq. (15). By plotting $\ln(1-K_d)$ vs $\ln(R_g)$ a linear relationship is obtained for each GPC column. The slope is $(3-d_P)$ and the intercept is $-(3-d_P)\ln L_P$. The obtained results are presented in Table IV.

The HR type column is filled with polystyrene–divinylbenzene particles having diameters of 5 μm. Based on the assumption that the fractal parameters d_G and L_G depends only on the diameter of the particles inside in the column, all the PS standards outside the intrapore separation regime (i.e., not selected in Table III) were used to determine these values. The relationship (7) may be rewritten as:

$$\ln(1 - K_d) = (3 - d_G)\ln(R_g) - (3 - d_G)\ln(L_G). \quad (17)$$

and the obtained plot of the data is presented in Figure 3. The slope equals $(3-d_G)$ and with a given d_G, L_G can be estimated from the y-axis segment.

The obtained linear relationship with data determined for three different columns is in perfect agree-

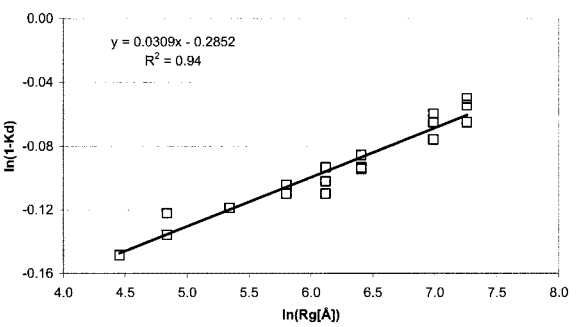

Figure 3 ln $(1 - K_d)$ vs ln $(R_g$ [Å]) in THF at 25°C for PS standards corresponding to interparticle separation regime (i.e., not selected in Table III).

ment with our prediction that d_G and L_G depends only on the packing particle diameter. By identification of the slope and intercept with the terms of relationship (17), we find: $d_G = 2.97$ and $L_G = 1$ μm. It is important to notice that the obtained value for d_G differs only by 1% from the value used in classical theory, $d_{G,\text{classical}} = 3$, which corresponds to no separation. Figure 3 shows unambiguously that this small difference is significant. The slope of $\ln(1-K_d)$ vs $\ln(R_g)$, identified as $(3-d_G)$, is 0.031 ± 0.002, clearly different from zero.

Once d_P, L_P, d_G, and L_G have been determined it is possible to calculate R_S for each column based on relationship (8). The results are listed in Table V.

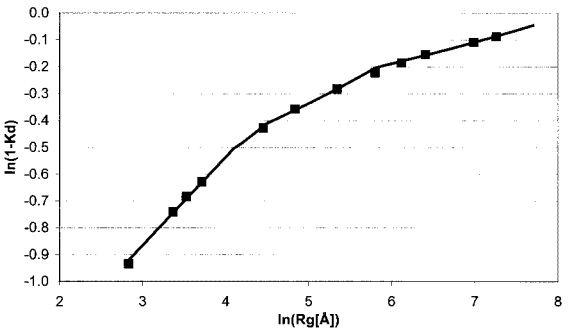

Figure 4 Experimental points (filled squares) obtained for the coupled set of columns of $\ln(1-K_d)$ vs $\ln(R_g[\text{Å}])$ and the predicted calibration curve (solid line) using the fractal parameters determined for each single column.

Column set calibration

For the coupled columns, the elution volume of each PS standard, recorded at the maximum of the peak, was used to calculate K_d based on relationship (9) and the corresponding V_0 and V_T values given in Table II. The experimental data are presented in Figure 4 together with the calculated (i.e., predicted) calibration curve based on eqs. (12) and (13) using the parameters determined for each chromatographic column listed in Tables II, IV, and V. We found an excellent agreement of the calculated curve with the experimental points.

CONCLUSIONS

We have extended the fractal theory for polymer fractionation in a GPC column to include the separation due to the interstitial space between gel particles. The developed model implies the characterization of the GPC column by five parameters with physical significance (V_P, d_P, L_P, d_G, and L_G), which are independent of the used chromatographic system. Based on the parameters measured for each column, the model allows the construction of the calibration curve for the column set.

We validated the model using 12 PS standards and a set of four columns. To correlate the experimental points of $\ln(1-K_d)$ vs $\ln(R_g)$ for PS standards with the constructed calibration curve, only one supplementary parameter that describes the chromatographic system, V_T, was necessary. Because V_T is the elution volume corresponding to the injected sample solvent, this value can be easily measured experimentally.

As a direct application, the obtained calibration curve allows the calculation of the absolute molecular mass for a polymer sample, for which Mark-Houwink constants are known.[19] Also, we find the model useful both for the development of new packs for chromatographic columns and for the choice of the columns to be coupled in a set. Thus, we give a theoretical base for the experimental known fact that for a good calibration curve, the selected columns must have particles with the same diameters. Moreover, L_G could be considered as the limiting value of the particles diameter that do not block the column. The obtained value of 1 μm confirms the need for prefiltering the sample solution before injection using filters having pores diameters of 0.45 μm.

The method also permits a direct evaluation of the gyration radius of the injected polymer samples. If the GPC system is equipped with a light-scattering detector, a rapid validation of the results can be performed by comparing the measured radius of gyration with the R_g values calculated based on column parameters.

TABLE V
R_S values for HR Columns

Column	R_S (nm)
HR2	5.9
HR3	9.0
HR4	33.6
HR5	217

References

1. Mandelbrot, B. The Fractal Geometry of Nature; Freeman Press: New York, 1982.
2. Gun'ko, V. M.; Do, D. D. Colloids Surf A, 2001, 193, 71.
3. Brown, C. A.; Siegmann, S. Int J Mach Tools Manufact 2001, 41, 1927.
4. Dathe, A.; Eins, S.; Niemeyer, J.; Gerold, G. Geoderma 2001, 103, 203.
5. Birdi, K. S. Fractals in Chemistry, Geochemistry, and Biophysics; Plenum Press: New York, 1993.
6. Duca, D.; Deganello, G. J Mol Catal A Chem 1996, 112, 413.
7. Chen, C.; Han, B.; Li, J.; Shang, J.; Zou, T.; Jiang, W. J Membr Sci 2001, 187, 109.
8. Meyers, J. J.; Crosser, O. K.; Liapis, A. I. J Chromatogr A 2001, 908, 35.
9. Kats, B. M.; Kutarov, V. V. Langmuir 1996, 12, 2762.

10. Hu, X.; Littrel, K.; Ji, S.; Pickles, D. G.; Risen, W. M., Jr. J Non-Cryst Solids 2001, 288, 184.
11. Hall, P. J.; Ruiz, M. W.; Gascon, G. D.; Barrientos, B. E.; Sherrington, D. C. J Chem Soc Faraday Trans 1996, 92, 2607.
12. Neimark, A. V.; Hanson, M.; Unger, K. K. J Phys Chem 1993, 97, 6011.
13. Casassa, E. F. J Polym Sci Part B 1967, 5, 773.
14. Casassa, E. F.; Tagami, Y. Macromolecules 1969, 2, 14.
15. Cassasa, E. F. J Phys Chem 1971, 75, 3929.
16. Casassa, E. F. Macromolecules 1976, 9, 182.
17. Brochard-Wyart, F.; LeMaire, M.; Ghazi, A.; Martin, M. In New Trends in Physics and Physical Chemistry of Polymers; Lieng-Huang Lee, Ed.; Plenum Press: New York, 1989.
18. Boborodea, A. G.; Clemens, M. L.; Stere, C.; Vasilescu, D. S. Polym Bull 2000, 44, 525.
19. ASTM D3593–80 Standard Test Method for Molecular Weight Averages and Molecular Weight Distribution of Certain Polymers by Liquid Size-Exclusion Chromatography, 1986.